Supporting Information

Enhancing proton conductivity in Zr-MOFs through tuning metal cluster connectivity

Guang-Rui Si,[a] Fan Yang,[b] Tao He,[a] Xiang-Jing Kong,[a] Wei Wu,[a] Tong-Chuan Li,[a] Kecheng Wang*[a] and Jian-Rong Li*[a]

[a] *Beijing Key Laboratory for Green Catalysis and Separation and Department of Environmental Chemical Engineering, Faculty of Environment and Life, Beijing University of Technology, Beijing 100124, P. R. Chin.*

[b] *State Key Laboratory of Membrane Separation and Membrane Processes, School of Chemistry and Chemical Engineering, Tiangong University, Tianjin,300387, P. R. Chin.*

E-mail: jrli@bjut.edu.cn

Section 1. Experiments

1. Materials and instruments

All reagents (AR grade) were commercially purchased and used as received without further purification. The ^{1}H NMR data were collected on a Bruker AVANCE III HD 400 MHz NMR spectrometer with tetramethylsilane as the internal standard. Fourier transform infrared (FT-IR) spectra were recorded on an IR Affinity-1 instrument (Shimadzu). The powder X-ray diffraction patterns (PXRD) were recorded on a Rigaku Smartlab3 X-ray Powder Diffractometer equipped with a Cu sealed tube (λ= 1.54178 Å) at room temperature. Simulation of the PXRD patterns was carried out by using the single-crystal data and diffraction-crystal module of the Mercury program, available free of charge at https://www.ccdc.cam.ac.uk/. TGA data were obtained on a TGA-50 thermogravimetric analyzer (Shimadzu) under an air atmosphere with the heating rate of 10 °C min^{-1}. Gas and vapor adsorption/desorption measurements were conducted on a BELSORP-Max instrument. Elemental analysis was performed by using a Vario Macro cube elementar. The morphologies were characterized by the scanning electron microscope (SEM, Hitachi-8020). The impedance measurements were performed using a Zennium electrochemical workstation.

2. Synthesis of $H_2BPDC(SO_3H)_2$

The ligand acid, 2,2′-disulfonyl-4,4′-biphenyldicarboxylic acid ($H_2BPDC(SO_3H)_2$) was synthesized using an improved reference method.[1]

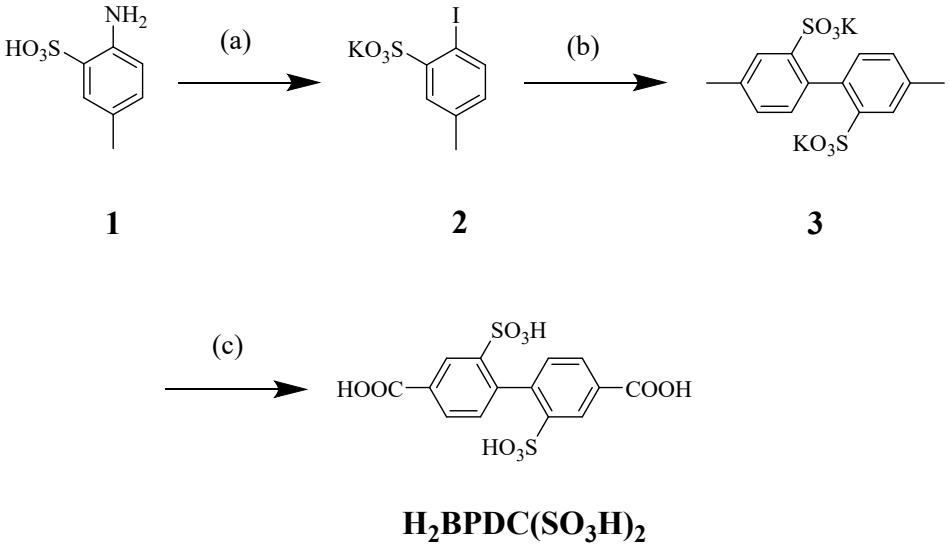

Scheme 1. The synthetic route of $H_2BPDC(SO_3H)_2$: (a) 36% HCl, KNO_2, KI, 25% H_2SO_4; (b) copper powder, $CuSO_4$, 90 °C for 5 h; (c) KOH, $KMnO_4$, 36 % HCl.

Synthesis of **2**: 4-aminotoluene-3-sulfonic acid (**1**, 30.0 g, 160.2 mmol), water (50 mL) and 36% hydrochloric acid (50 mL) were added to a reaction flask. The mixture was stirred and cooled to 0 °C. A solution of potassium nitrite (14.7 g, 173.4 mmol) in water (20 mL) was added slowly. Then the mixture was stirred for 2 h at 0 °C. A dark wet mass was filtered off and then was added in portions into a solution containing potassium iodide (39.9 g, 240 mmol) dissolved in 25% sulfuric acid (100 mL) at 0 °C. Then the ice water bath was removed, 25% solution of sulfuric acid (100 mL) was added, and stirring was continued at 70 °C for 45 min. After completion of the reaction, the mixture was hot filtered from black solids, and crystallization was facilitated by cooling in an ice bath. The precipitate was filtered off, thoroughly washed once with ethanol-water 1:1 (50 mL) and ethanol (50 mL), and dried at 80 °C to afford **2** as a brown solid (29.8 g, 55.4% based on **1**).

Synthesis of **3**: To a mixture of **2** (21.6 g, 0.47 mmol) in water (80 mL) was added an aqueous solution containing copper sulfate (0.118 g, 0.235 mmol) in water (20 mL). After the mixture was stirred for 15 min at 90 °C, 6.0 g of copper powder (91.8 mmol) was added in one portion. Then stirring was continued for 5 h at 90°C. After completion of the reaction, the mixture was filtered, the solution was concentrated on

a rotary evaporator until the total volume was approximately 20 mL, and ethanol (15 mL) was added dropwise. The powdery product was filtered off, thoroughly washed two times with ethanol-water 3:1 (20 mL), and dried at 80 °C to afford **3** as a white solid (17.5 g, 65.1% based on **2**).

Synthesis of **$H_2BPDC(SO_3H)_2$**: Potassium hydroxide (6.4 g, 114.0 mmol) was added to a solution of **3** (9.2 g, 22.0 mmol) in water (150 mL) and methanol (10 mL). The mixture was heated to 55 °C, and potassium permanganate (22.0 g, 139.2 mmol) was added in portions for 3 hours. The reaction mixture was refluxed for 24 h with vigorous stirring. After completion of the reaction, the heterogeneous brown mixture was hot filtered with diatomite to give a clear solution. The solvent was removed in vacuo until the total volume was approximately 20 mL, and the residue was acidized with hydrochloric acid (20 mL). The resulting white precipitate was filtered, washed two times with ethanol-water 4:1 (20 mL) and then was dissolved in 30 mL water. To the mixture, perchloric acid (72%, 3 mL) was added slowly with stirring. After the insoluble solid was filtrated off, the resulting clear solution was evaporated to 3 mL at a reduced pressure and cooled in an ice bath, the white product was filtered off, washed once with ice-water and twice with ethanol, and dried at 80 °C to afford **$H_2BPDC(SO_3H)_2$** as a white solid (3.76 g, 42.5% based on **3**). ^{1}H NMR (DMSO-d_6, 400 MHz): δ = 8.44 (d, 2H), 7.74-7.76 (m, 2H), 7.40 (d, 2H) (Fig. S1).

3. Synthesis of BUT-76/77 and BUT-77@PP membrane

Crystal blocks of BUT-76 ($Zr_6O_4(OH)_8(H_2O)_4(BPDC(SO_3H)_2)_4$): $ZrOCl_2{\cdot}8H_2O$ (15 mg, 0.047 mmol) and $H_2BPDC(SO_3H)_2$ (10 mg, 0.025 mmol) were dissolved in 2 mL of DMF under ultrasound in a 4 mL glass vial. 200 μL of trifluoroacetic acid were added to the solution. The vial was sealed and heated at 120 °C for 96 h. After being cooled to room temperature, the resulting colorless crystals of BUT-76 were collected by filtration, washed with DMF and methanol, and then dried under reduced pressure at room temperature. (2.1 mg, 14% yield based on the $H_2BPDC(SO_3H)_2$ ligand).

Bulk powders of BUT-76: $ZrOCl_2{\cdot}8H_2O$ (150 mg, 0.465 mmol) and

$H_2BPDC(SO_3H)_2$ (100 mg, 0.249 mmol) were dissolved in 15 mL of DMF in a 40 mL high-pressure vessel. To the solution trifluoroacetic acid (1 mL) was added. The vessel was then tightly sealed and the mixture was heated in an oil bath of 120 °C for 12 h with stirring. After cooling down to room temperature, the white solid (113 mg of activated sample, 76% yield based on the $H_2BPDC(SO_3H)_2$ was collected by filtration, and washed with DMF (2 × 10 mL), methanol (3 × 10 mL) and dried under reduced pressure at room temperature. Elemental analysis for BUT-76 ($Zr_3C_{28}O_{28}S_4H_{12}$) after activation and evacuation: Calc. C 28.04, H 1.00, S 10.70. Found. C 27.95, H 1.12, S 10.35.

Bulk powders of BUT-77 ($Zr_6O_4(OH)_8(H_2O)_4(BPDC(SO_3H)_2)_4$): $ZrOCl_2{\cdot}8H_2O$ (150 mg, 0.465 mmol) and $H_2BPDC(SO_3H)_2$ (100 mg, 0.249 mmol) were dissolved in 15 mL of DMF in a 40 mL high-pressure vessel. To the solution acetic acid (6 mL) was added. The vessel was then tightly sealed and the mixture was heated in an oil bath of 140 °C for 12 h with stirring. After cooling down to room temperature, the white solid (78 mg of activated sample, 61% yield based on the $H_2BPDC(SO_3H)_2$ was collected by filtration, and washed with DMF (2 × 10 mL), methanol (3 × 10 mL) and dried under reduced pressure at room temperature. Elemental analysis for BUT-77 ($Zr_3C_{42}O_{34}S_6H_{32}$) after activation and evacuation: Calc. C 32.58, H 2.07, S 12.43. Found. C 32.42, H 2.12, S 12.35.

BUT-77@PP membrane: The membrane was synthesized using an improved reference method.[2] BUT-77 (80 mg) was sonically dispersed in the DMF (5 mL) for 2 hours. Subsequently, PVDF (M_w = 534000) (120 mg) and PVP (M_n = 360000) (280 mg) were added into the above dispersion and then the mixture was stirred at room temperature for 5 hours to get a homogeneous jelly, which was poured onto a glass petri dish, which was dried under at 80 °C for 12 h for removing DMF. When the temperature dropped to room temperature, the membrane was removed from the petri dish dried in a vacuum oven at 80 °C for 24 h for further investigations.

4. Single-crystal X-ray diffraction

Crystals were taken from the mother liquid without further treatment, transferred to oil and mounted into a loop for single-crystal X-ray data collection. Single-crystal X-ray diffraction data were collected on an Agilent Supernova CCD diffractometer equipped with a micro-focus sealed Supernova (Cu-*Kα)* X-ray Source (λ= 1.54178 Å) at room temperature. The data were corrected by empirical absorption correction using spherical harmonics, implemented in the SCALE3 ABSPACK scaling algorithm. The structure was solved by direct methods and refined by full-matrix least-squares on F^2 with anisotropic displacement by using the Olex2 software package. In this structure, sulfonate possesses highly disorders and was treated by using a Fragment DB routine in the Olex2 software package.[3] Hydrogen atoms of ligands were solved in ideal positions with isotropic displacement parameters. Those in H_2O molecules coordinated to the Zr(IV)-based node were not added but were calculated into the molecular formula. All non-hydrogen atoms were refined anisotropically during the final cycle. Large solvent accessible pores in BUT-76 and BUT-76w were occupied by highly disordered solvent molecules. The details of data collection and structural refinement are summarized in Table S1.

5. Rietveld refinement for BUT-77

To confirm the structures of BUT-77, the pattern matching analysis were carried out for BUT-77 by the rietveld refinement.[4] By comparing the calculated and experimental pattern, the final fit shows very good agreement with the parent UiO-67, which suggests that BUT-77 is composed of the similar framework structure to that of UiO-67. The detail data are illustrated in Table S2 and the PXRD pattern are shown in Figure S2.

6. Stability test

MOF samples (20 mg for each batch) were treated with 50 mL different acid/alkaline aqueous solutions at room temperature for 24 h, respectively. The samples collected after treatments were immersed in methanol for further investigations.

7. Sample activation and gas/vapor adsorption

Before gas/vapor adsorption measurements, samples of BUT-77 and -76 powder (about 80 mg for each) were soaked in 200 mL of DMF for 24 h at 60 °C. Next, DMF was decanted and the MOF samples were immersed in 40 mL methanol in the autoclave at 80 °C for two days with replacing the soaking solvent every 12 h. After solvent exchange, the samples were collected by centrifugation and dried under vacuum. Before adsorption measurements, the samples were loaded in a sample tube and degassed at an optimal temperature of 100 °C for 12 h. The N_2, CO_2 and vapor adsorption measurements were conducted at 77 K in a liquid N_2 bath, 195 K in dry ice-acetone bath and 298 K in a water bath, respectively. For recycling vapor adsorption experiments, the samples were degassed under vacuum at 100 °C for 12 h for next run. Before proton conductivity measurement, the samples were further dried for 12 h at 100 °C.

8. Proton conduction measurement

The activation MOF powder (80-100 mg) was pressed under 1000 kg cm^{-2} pressure for 2 min to make a plate (length 1.0 cm and width 0.4 cm). Both sides of the plate were attached to silver wires with silver paste and then put in a sealed double-walled glass chamber. The relative humidity (RH) inside the chamber was controlled by standard saturated aqueous solutions of KCl, NaCl, $NaNO_2$, $Mg(NO_3)_2$, and $MgCl_2$ (corresponding RH are about 85, 75, 65, 53, and 33%, respectively).[5] The proton conductivities of the plate were then tested by a quasi-four-probe method in the chamber connected with a temperature controlled circulation water bath. The impedance measurements were carried out by using a Zennium electrochemical workstation with tuned frequencies from 1 Hz to 4 MHz and alternating potentials of 100 mV. As for the membrane sample, it was cut into a rectangle and sandwiched between two gold pieces. The proton conductivity (σ, S cm^{-1}) of the sample was estimated by using the equation (1):

$$\sigma = L / (RA) \qquad (1)$$

where L (cm) is the length of the block, R (Ω) is the impedance, and A (cm^2) is the face area of the plate (A = thickness × width). All measurements were repeated three times to get reproducible results.

The activation energy (E_a) was calculated by the equation (2) in previous literature.

$$\sigma = \frac{\sigma^0}{kT} exp(\frac{-E_a}{kT}) \quad (2)$$

where σ^0 is a constant, k is the Boltzmann constant, T is the temperature (K), E_a is the activation energy (eV).

9. Gas permeation test

A constant-volume permeation system was implied to assess single gas permeability at 35 °C. Before measurement, the membrane was masked with impermeable aluminum tape with a hole in the center and the interface of tape was covered with a Duralco™ 4525 epoxy (Cotronics Corp.). The system was evacuated overnight to remove volatile gases, followed by testing downstream leak rate (typically ≤ 10^{-6} torr/s). The change in downstream pressure with time was monitored via LabView software until a steady state was achieved. The pure gas permeability (P) of the membrane, in-unit of Barrer (1 Barrer = 10^{-10} cm^3 (STP) cm/cm^2 s cm Hg), was calculated by the following equation:

$$P = \frac{V_d L}{P_2 ART} \times \frac{dp}{dt}$$

where P represents the permeability (cm^3 (STP) cm/cm^2 s cm Hg), dp/dt is the slope of the downstream pressure vs. time (Torr/sec); L is the thickness of the membrane (μm, measured with a digital micrometre (Mitutoyo) at different locations within each membrane and then averaged.); V_d is the downstream volume of permeation system (cm^3); A is the membrane area (cm^2); T is the testing temperature (K).

10. Molecular Simulation

The Grand Canonical Monte Carlo simulations (GCMC) were performed for water adsorption on BUT-76 and -77 at 100 kPa and 298 K. The crystal structure of BUT-76w determined by single-crystal X-ray analysis was used for the accurate simulation. The interactions between the guest water molecules and the MOF structures were described by site-to-site Lennard-Jones (LJ) contributions. Water molecules were modeled by the three-point transferable interaction potentials (TIP3P) model.[6] The dispersive and steric repulsive interactions of each atoms in BUT-76w and -77 frameworks and water molecules were both modeled by the dreiding force field (Dreiding) or universal force field (UFF).[7] The QEq method was used to equilibrate and redistribute the overall charge of atoms of the MOF structures. Electrostatic interaction was evaluated through Ewald summation method. The cutoff distance was set at 12.5 Å. 20000000 Monte Carle steps were constructed to simulate the favorable adsorption sites, in which the first 10000000 steps were for equilibration and the remains were production steps. All the simulations were carried out by using sorption module in the Material Studio software.[8]

Section 2. General Characterizations

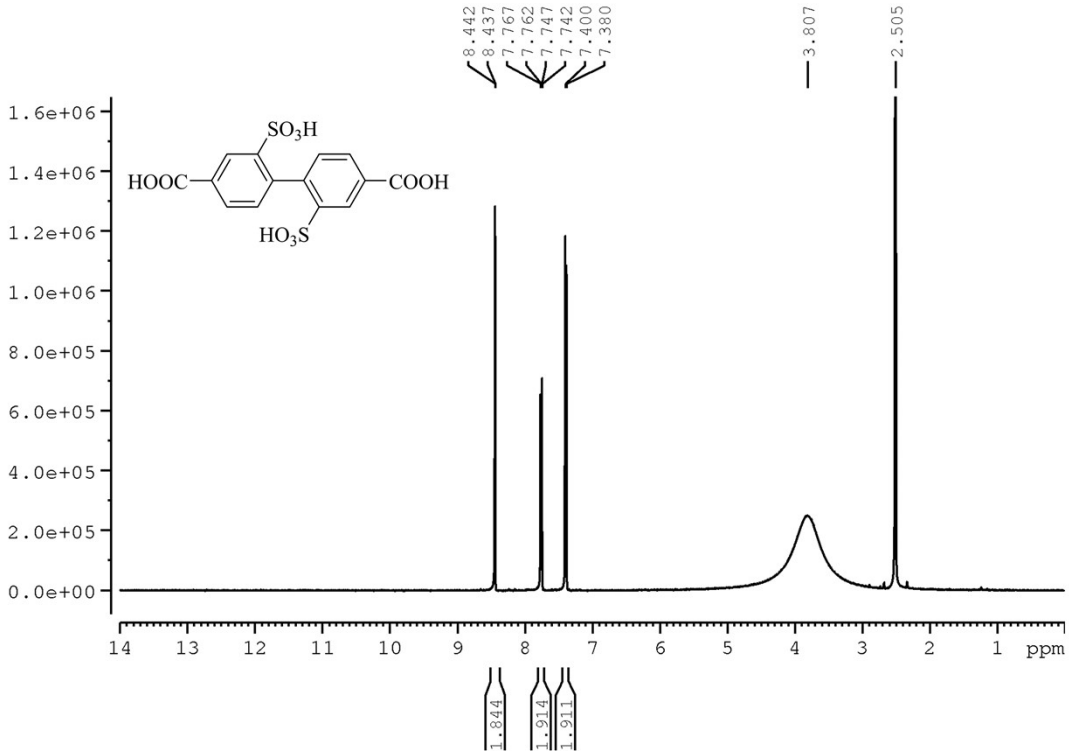

Fig. S1. ^{1}H NMR spectrum of **$H_2BPDC(SO_3H)_2$**.

Table S1. The crystallographic data for BUT-76 and -76w.

MOF	BUT-76	BUT-76w
CCDC Number	2060505	2102688
Crystal system	Tetragonal	Tetragonal
Space goup	$P4_2/mmc$	$P4_2/mmc$
a/ Å	22.7520(3)	24.3846(8)
b/ Å	22.7520(3)	24.3846(8)
c/ Å	19.1914(8)	14.2726(14)
α/ (°)	90	90
β/ (°)	90	90
γ/ (°)	90	90
V/ Å^3	9934.5(5)	8486.6(10)
λ/ Å	1.54178	1.54178
Absorption correction type	multi-scan	multi-scan
Goodness-of-fit on F^2	1.166	1.143
R_1[a], wR_2[b] [$I>2\sigma(I)$]	R_1 = 0.0854, wR_2 = 0.2741	R_1 = 0.1287, wR_2 = 0.3617
R_1[a], wR_2[b] (all data)	R_1 =0.1150, wR_2 = 0.3068	R_1 =0.1895, wR_2 = 0.4200

[a] $R_1 = \Sigma||F_o|-|F_c|| / \Sigma|F_o|$

[b] $wR_2 = \{\Sigma[w(F_o^2 - F_c^2)^2] / [w(F_o^2)^2]\}^{1/2}$, $[F_o>4\sigma(F_o)]$

Table S2. The pattern matching analysis data for BUT-77.

BUT-77 (CCDC number: 2116259)		
Initial lattice parameter	a = 26.9183(7) Å	α = 90 °
	b = 26.9183(7) Å	β = 90 °
	c = 26.9183(7) Å	γ = 90 °
	V = 19504.8(9) Å^3	
Fitted lattice parameter	a = 26.8988(12) Å	α = 90 °
	b = 26.8988(12) Å	β = 90 °
	c = 26.8988(12) Å	γ = 90 °
	V = 19462.6(15) Å^3	
R_p	8.29%	
R_{wp}	10.9 %	

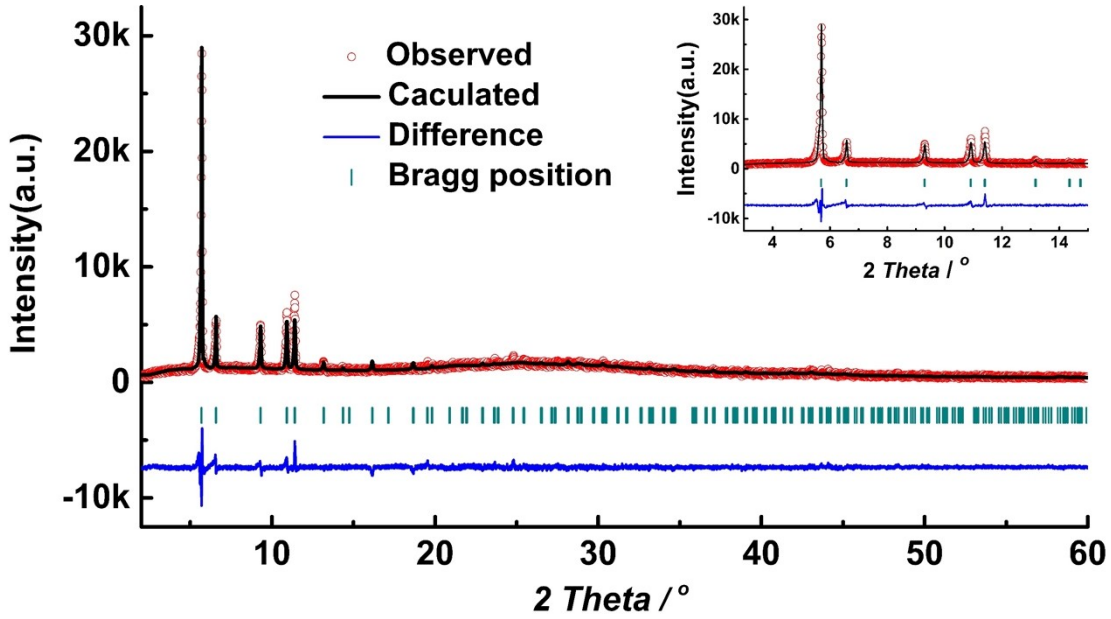

Fig. S2. Rietveld refinement method fit to PXRD data for BUT-77.

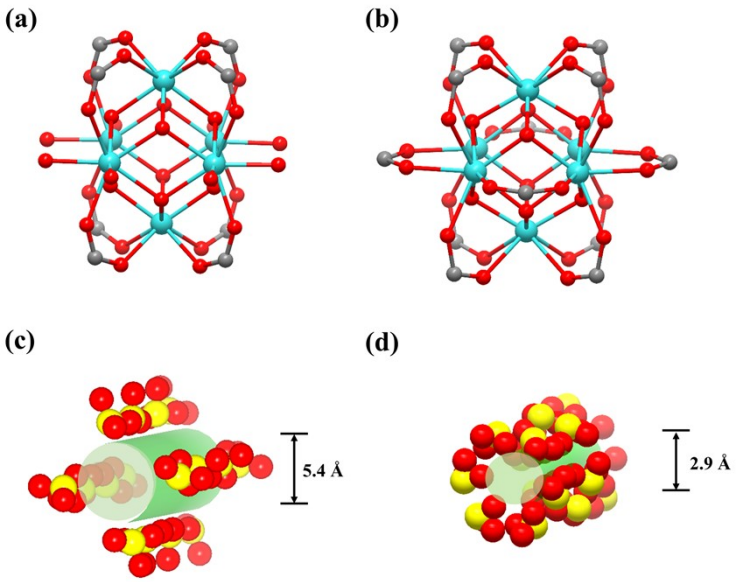

Fig. S3. Representations of the 8-connected zirconium clusters and 12-connected clusters (a) (b); Channels functionalized by sulfonate groups in BUT-76 (c) and -77 (d).

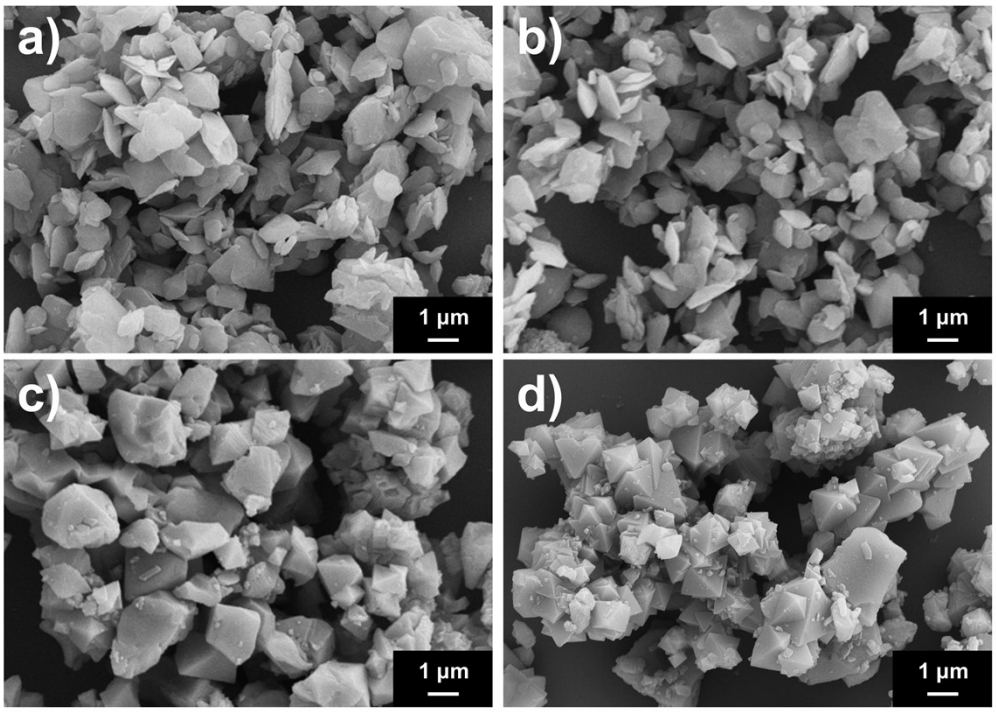

Fig. S4. SEM images of BUT-76 and -77 for the crystalline powders before (a) (c) and after (b) (d) water measurement.

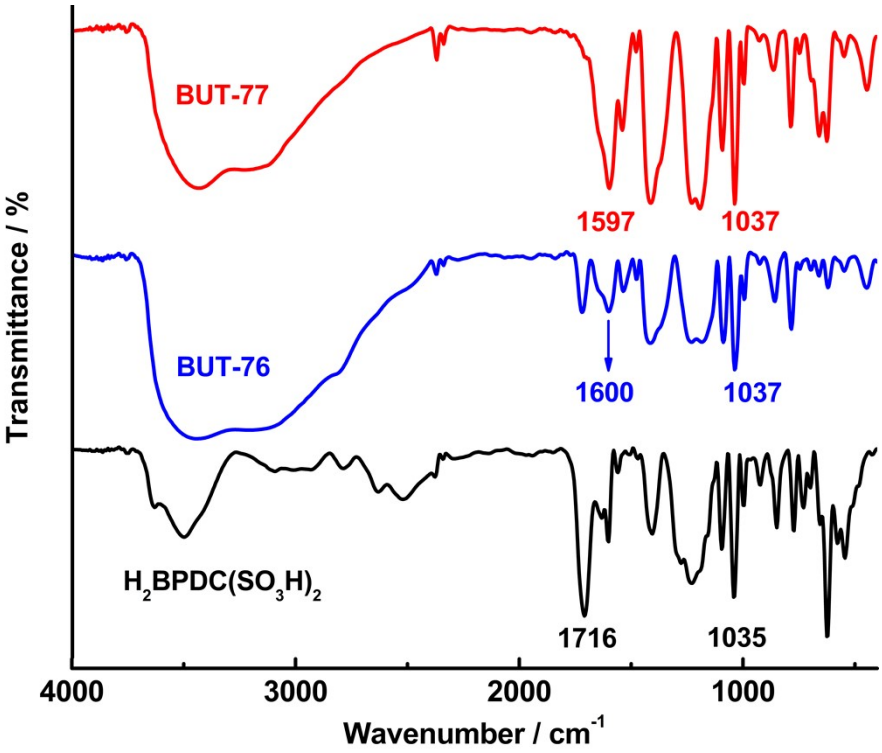

Fig. S5. FT-IR spectra of $H_2BPDC(SO_3H)_2$, BUT-76 sample and -77.

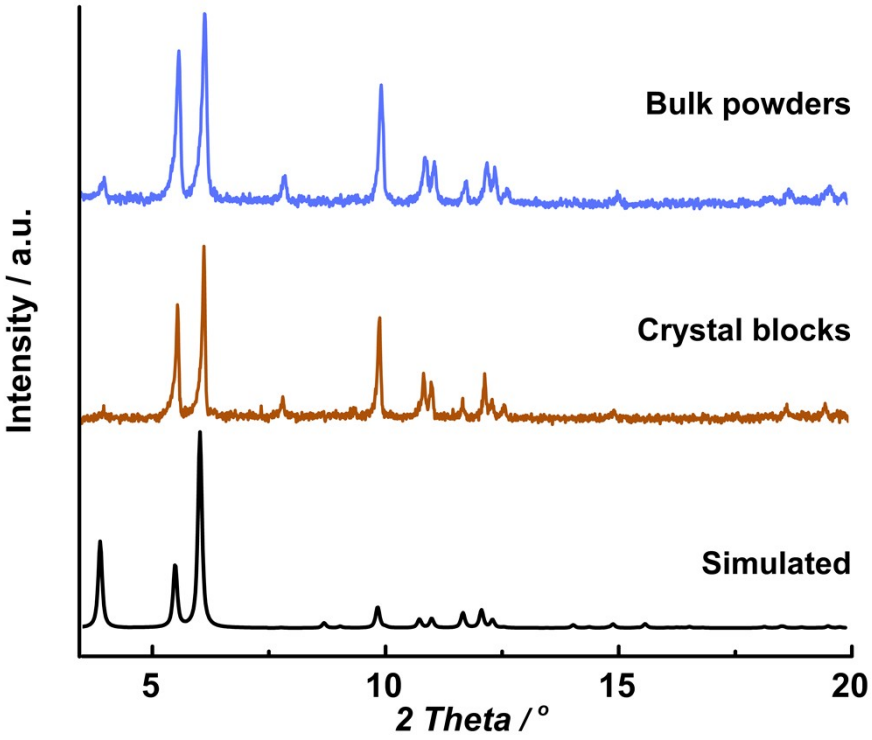

Fig. S6. PXRD patterns of bulk powders and crystal blocks of BUT-76.

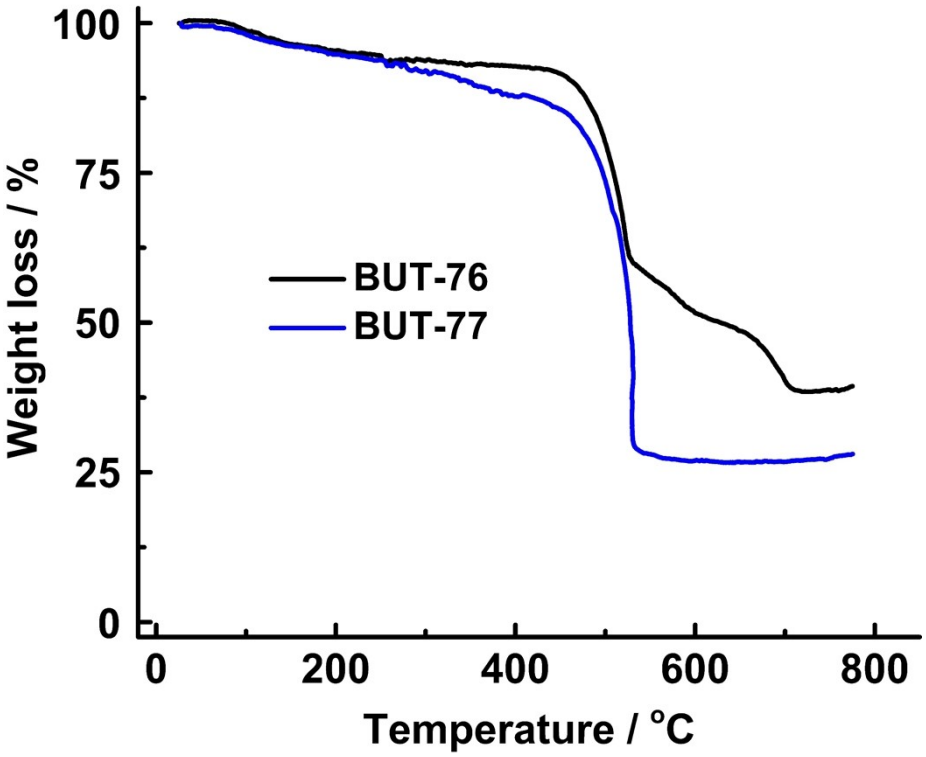

Fig. S7. TGA curves of activated BUT-76 and -77.

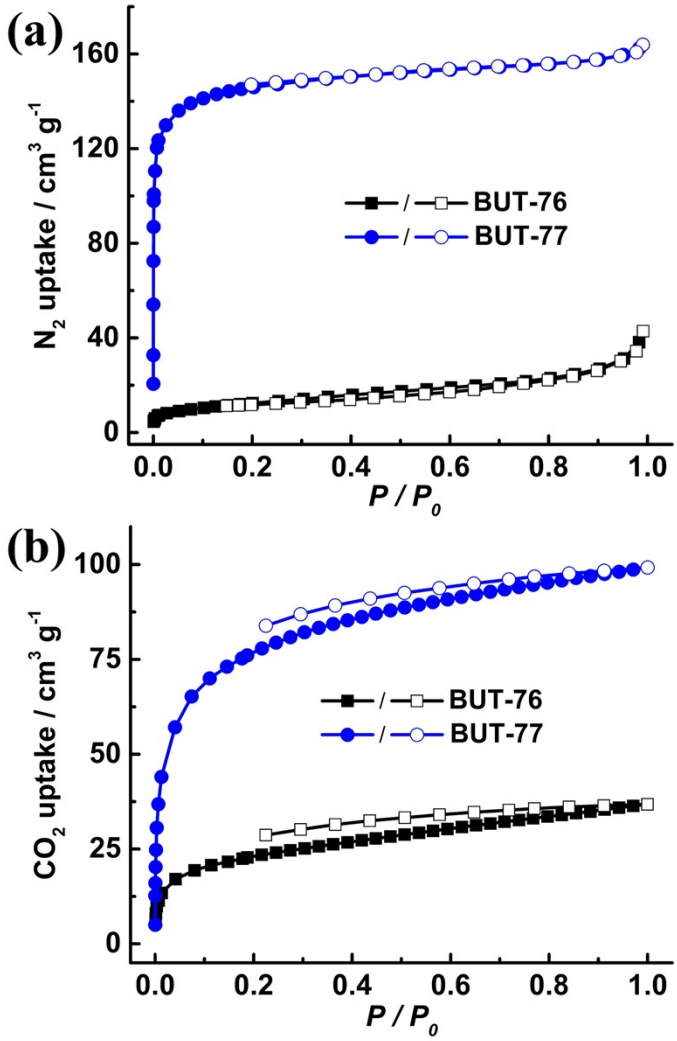

Fig. S8. N_2 and CO_2 adsorption/desorption isotherms of BUT-76 and BUT-77 at 77 and 195 K.

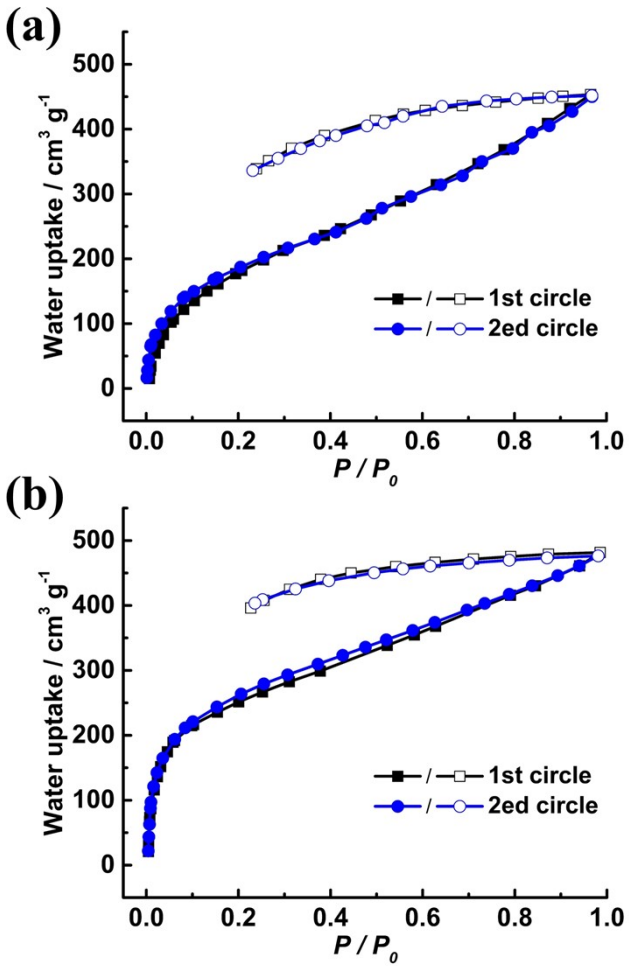

Fig. S9. Water cycling vapor adsorption/desorption isotherms of BUT-76 (a) and -77 (b) at 298 K.

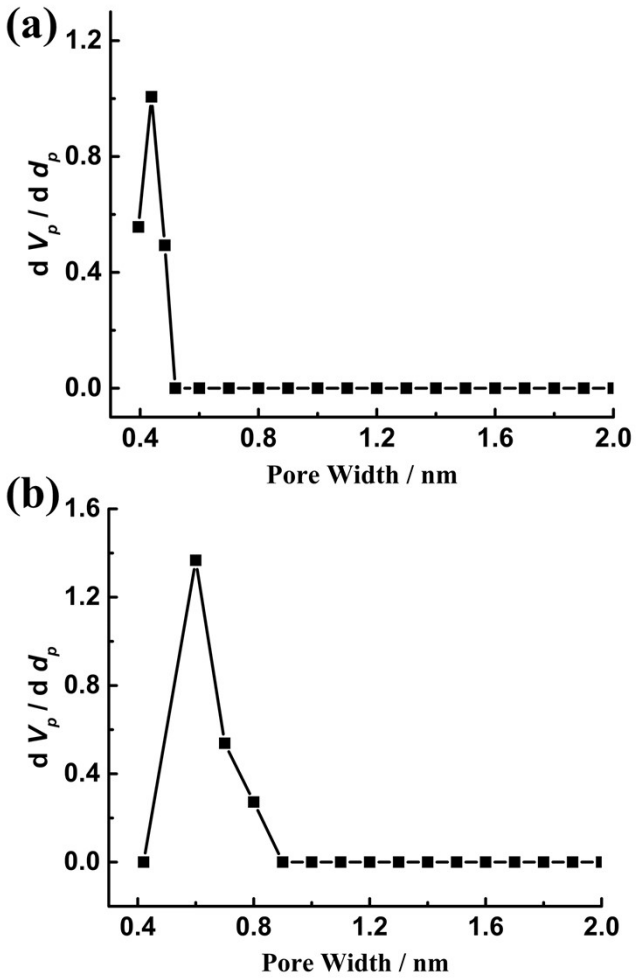

Fig. S10. Pore size distribution evaluated by using the N_2 adsorption data for BUT-76 (a) and -77 (b).

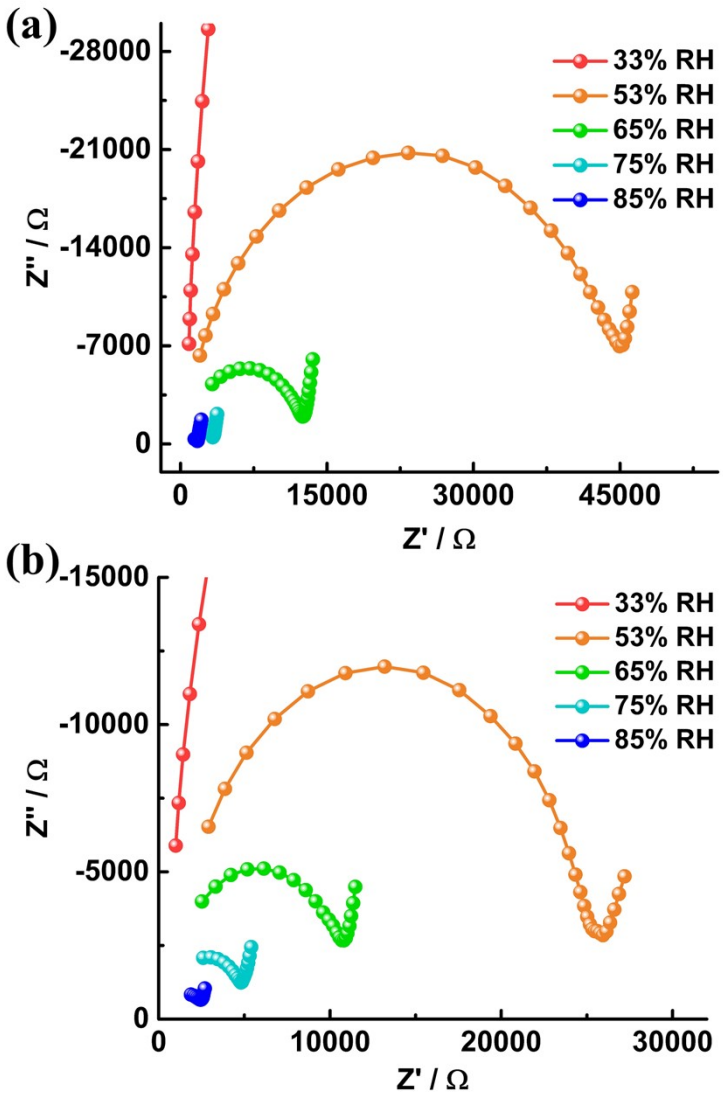

Fig. S11. Humidity-dependent impedance plots of BUT-76 (a) and -77 (b) at 33~85% RH.

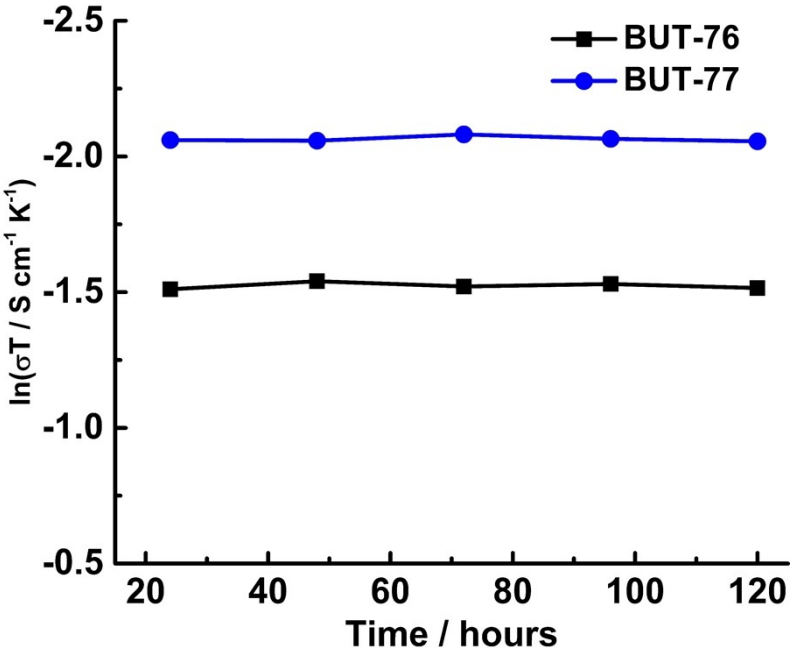

Fig. S12. Time-dependent proton conductivities of BUT-76 and -77 at 80 °C and 100% RH.

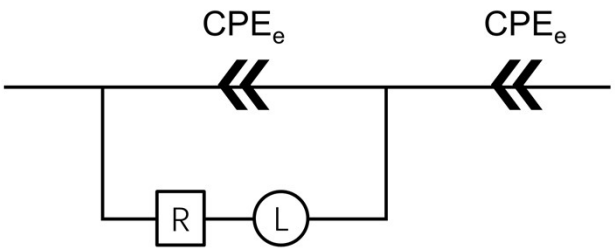

Fig. S13. The used equivalent circuit for fitting AC impedance plots.

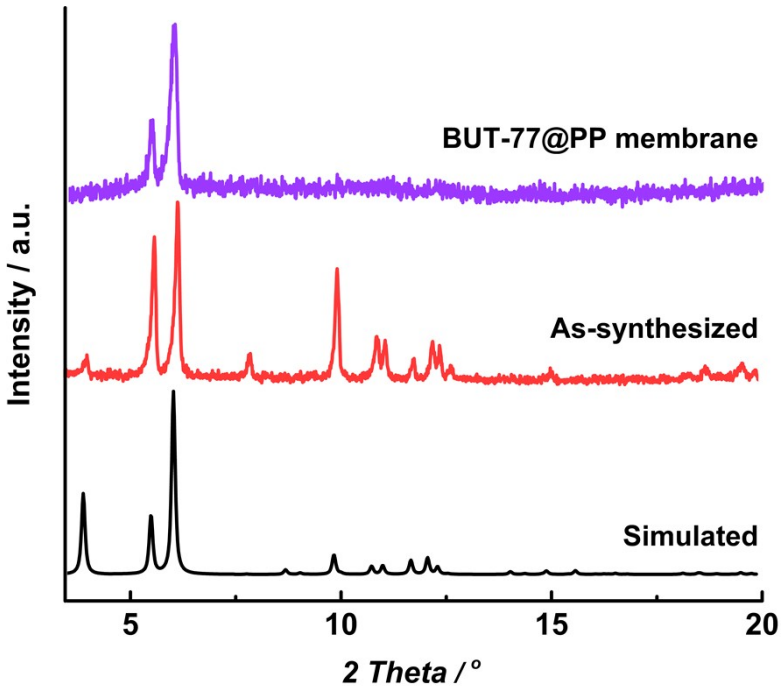

Fig. S14. PXRD patterns of as-synthesized BUT-77 samples (red) and BUT-77@PP membrane (purple).

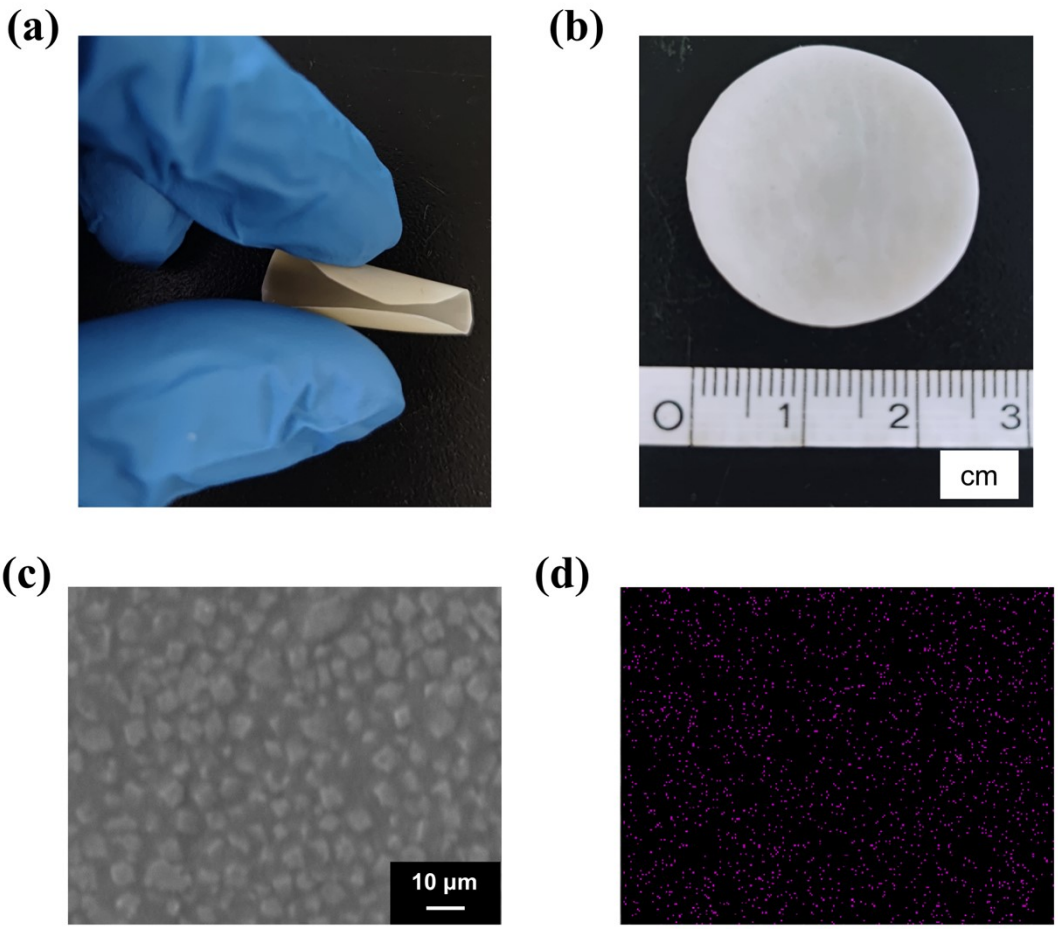

Fig. S15. Optical images (a and b) and SEM images (c) of BUT-77@PP membrane and the elemental mapping image (d) of Zr in BUT-77@PP membrane.

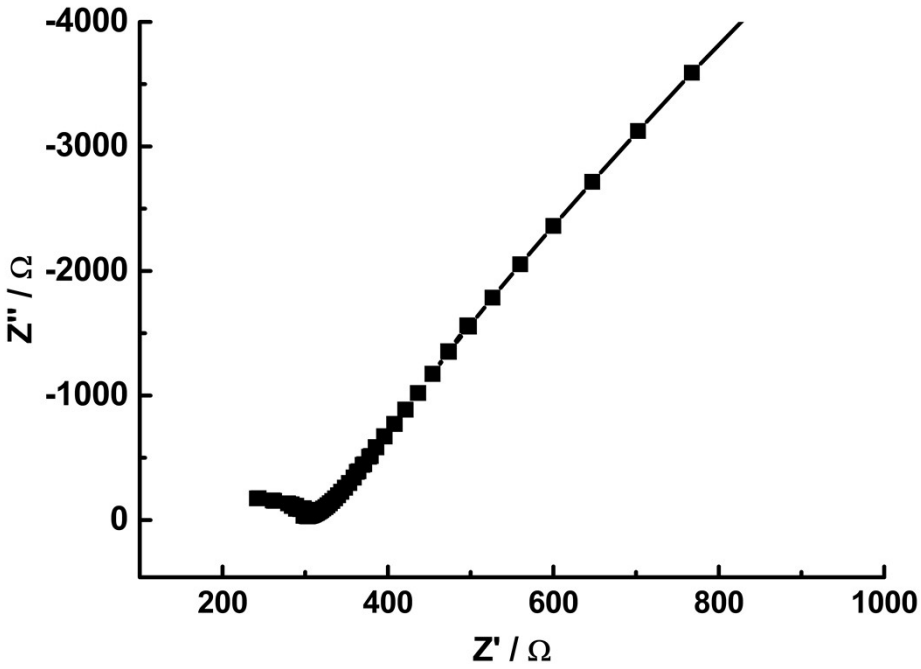

Fig. S16. Impedance plot of BUT-77@PP membrane at 80 °C and 100% RH.

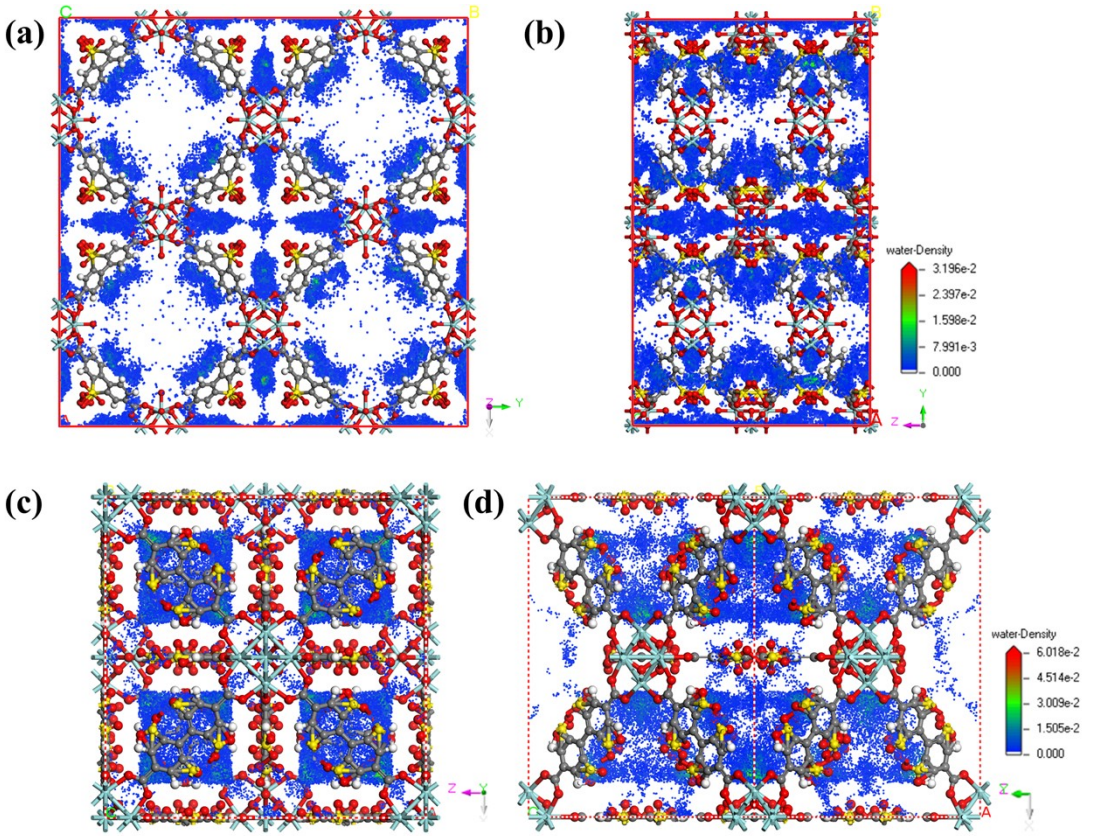

Fig. S17. The water density profiles from GCMC simulations of BUT-76 (a-b) and -77 (c-d).

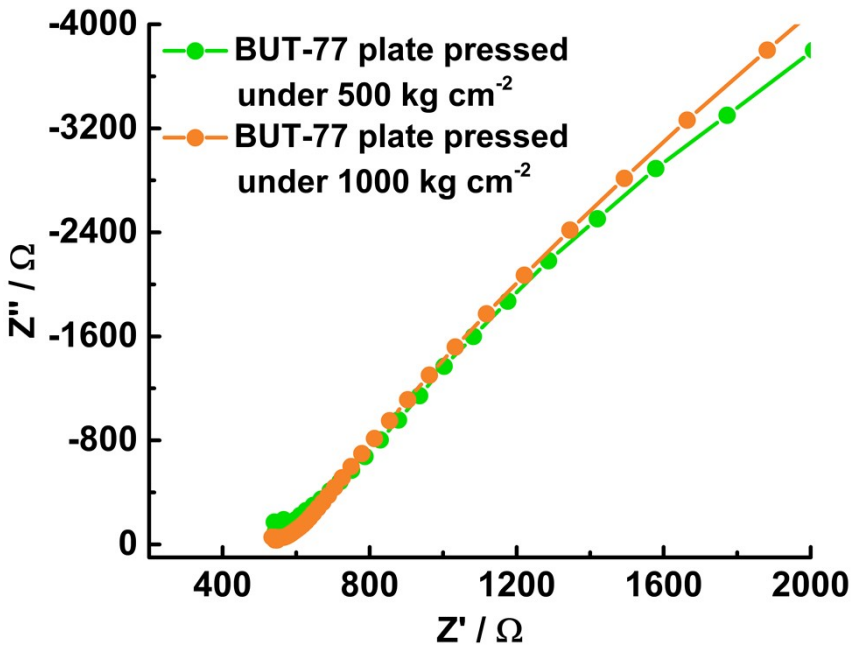

Fig. S18. Impedance plots of BUT-77 samples pelletized under 500 and 1000 kg cm^{-2} pressure at 80 °C and 100% RH.

Table S4. Proton conductivities of selected Zr-MOFs

Compounds	Conductivity (S cm^{-1})	T (°C)	RH (%)	Ref.
UiO-66	7.54×10^{-6}	30	97	9
UiO-66-Br	2.23×10^{-7}	30	97	9
UiO-66-NH_2	1.40×10^{-5}	30	97	9
UiO-66-SO_3H	3.40×10^{-3}	30	97	9
UiO-66-2COOH	1.0×10^{-3}	30	97	9
UiO-66-$(SH)_2$	4.3×10^{-6}	80	90	10
Him@UiO-67	1.52×10^{-3}	130	-	11
Zr-bpdc-4SO_2Me4F	1.75×10^{-4}	100	98	12
MOF-808-ox	4.25×10^{-4}	80	98	13
Him11@VNU-17	5.93×10^{-3}	70	98	14
His8.2@VNU-23	1.79×10^{-2}	95	85	15
Zr-BTNDC-ox	4.03×10^{-3}	95	95	16
$((Me)_2NH_2)_2[Li_2Zr(ox)_4]$	3.9×10^{-5}	17	67	17
MIP-202(Zr)	1.1×10^{-2}	90	95	18
MOF-801	1.88×10^{-3}	25	98	19
1_lp@H	5.4×10^{-5}	80	95	20
1_np@H	6.6×10^{-5}	80	95	20
ZPGly	1×10^{-3}	140	95	21
PCMOF20	1×10^{-2}	80	95	22
ZrPP-1	8.0×10^{-3}	25	98	23
ZrPP-2	4.2×10^{-3}	25	98	23
MIL-163	2.1×10^{-3}	90	95	24
BUT-76	**8.55×10^{-3}**	**80**	**100**	**This work**
BUT-77	**3.08×10^{-2}**	**80**	**100**	**This work**

Section 3. References

1. J. Zhao, X. He, Y. Zhang, J. Zhu, X. Shen and D. Zhu, Cryst. Growth Des., 2017, **17**, 5524.

2. (a) X.-M. Li, J. Liu, C. Zhao, J.-L. Zhou, L. Zhao, S.-L. Li and Y.-Q. Lan, J. Mater. Chem. A, 2019, **7**, 25165; (b) J. Zhang, H.-J. Bai, Q. Ren, H.-B. Luo, X.-M. Ren, Z.-F. Tian and S. Lu, ACS Appl. Mater. Interfaces, 2018, **10**, 28656; (c) Z. Guo, X. Xu, Y. Xiang, S. Lu and S. P. Jiang, *J. Mater. Chem. A*, 2015, **3**, 148.

3. O. V. Dolomanov, L. J. Bourhis, R. J. Gildea, J. A. K. Howard and H. Puschmann, *J. Appl. Crystallogr.*, 2009, **42**, 339.

4. P. W. Stephens, *Dordrecht*, 2012.

5. X. Liang, F. Zhang, W. Feng, X. Zou, C. Zhao, H. Na, C. Liu, F. Sun and G. Zhu, *Chem. Sci.*, 2013, **4**, 983.

6. W. L. Jorgensen, J. Chandrasekhar, J. D. Madura, R. W. Impey and M. L. Klein, *J. Chem. Phys.*, 1983, **79**, 926.

7. A. K. Rappe, C. J. Casewit, K. S. Colwell, W. A. Goddard and W. M. Skiff, *J. Am. Chem. Soc.*, 1992, **114**, 10024.

8. B. Delley, *J. Chem. Phys.*, 2000, **113**, 7756.

9. F. Yang, H. Huang, X. Wang, F. Li, Y. Gong, C. Zhong and J.-R. Li, *Cryst. Growth Des.*, 2015, **15**, 5827.

10. W. J. Phang, H. Jo, W. R. Lee, J. H. Song, K. Yoo, B. Kim and C. S. Hong, *Angew. Chem., Int. Ed.*, 2015, **54**, 5142.

11. S. Liu, Z. Yue and Y. Liu, *Dalton Trans.*, 2015, **44**, 12976.

12. W.-R. Xian, Y. He, Y. Diao, Y.-L. Wong, H.-Q. Zhou, S.-L. Zheng, W.-M. Liao, Z. Xu and J. He, *Inorg. Chem.*, 2020, **59**, 7097.

13. X. Meng, H.-N. Wang, L.-S. Wang, Y.-H. Zou and Z.-Y. Zhou, *CrystEngComm*, 2019, **21**, 3146.

14. T. H. N. Lo, M. V. Nguyen and T. N. Tu, *Inorg. Chem. Front.*, 2017, **4**, 1509.

15. M. V. Nguyen, T. H. N. Lo, L. C. Luu, H. T. T. Nguyen and T. N. Tu, *J. Mater. Chem. A*, 2018, **6**, 1816.

16. Q. Zeng, W.-R. Xian, Y.-H. Zhong, L.-H. Chung, W.-M. Liao and J. He, *J. Solid State Chem.*, 2020, **285**, 121234.

17. S. Tominaka, F. Coudert, T. D. Dao, T. Nagao and A. K. Cheetham, *J. Am. Chem. Soc.*, 2015, **137**, 6428.

18. S.-J. Wang, M. Wahiduzzaman, L. Davis, A. Tissot, W. Shepard, J. Marrot, C. Martineau-Corcos, D. Hamdane, G. Maurin, S. Devautour-Vinot and C. Serre, *Nat. Commun.*, 2018, **9**, 4937.

19. J. Zhang, H.-J. Bai, Q. Ren, H.-B. Luo, X.-M. Ren, Z.-F. Tian and S.-F. Lu, *ACS*

Appl. Mater. Interfaces, 2018, **10**, 28656.
20. F. Costantino, A. Donnadio and M. Casciola, *Inorg. Chem.*, 2012, **51**, 6992.
21. A. Donnadio, M. Nocchetti, F. Costantino, M. Taddei, M. Casciola, F. da Silva Lisboa and R. Vivani, *Inorg. Chem.*, 2014, **53**, 13220.
22. Z. H. Fard, N. E. Wong, C. D. Malliakas, P. Ramaswamy, J. M. Taylor, K. Otsubo and G. K. H. Shimizu, *Chem. Mater.*, 2018, **30**, 314.
23. E.-X. Chen, G. Xu and Q. Lin, *Inorg. Chem.*, 2019, **58**, 3569.
24. P. G. M. Mileo, S. Devautour-Vinot, G. Mouchaham, F. Faucher, N. Guillou, A. Vimont, C. Serre and G. Maurin, *J. Phys. Chem. C*, 2016, **120**, 24503.